

Enhancements of Spin and Orbital Magnetic Moments of Submonolayer Co on Cu(001) Studied by X-ray Magnetic Circular Dichroism Using Superconducting Magnet and Liquid He Cryostat

Takeshi NAKAGAWA, Yasumasa TAKAGI, Yoshihiro MATSUMOTO¹, and Toshihiko YOKOYAMA

Department of Materials Molecular Science, Institute for Molecular Science and Department of Structural Molecular Science,
The Graduate University for Advanced Studies (Sokendai), Okazaki, Aichi 444-8585, Japan

¹Advanced Science Research Center, Japan Atomic Energy Institute, Tokai, Ibaraki 319-1195, Japan

(Received October 4, 2007; revised November 13, 2007; accepted December 18, 2007; published online April 18, 2008)

Magnetic properties of 0.4 monolayer Co grown epitaxially on Cu(001) were investigated by X-ray magnetic circular dichroism (XMCD) using our newly constructed ultrahigh vacuum system equipped with a 7 T superconducting magnet and a liquid He cryostat. The angle-dependent XMCD spectra for the saturated magnetization recorded at 6.0 K allowed us to evaluate separately the spin and orbital magnetic moments along the surface parallel and normal directions. Enhancements of the magnetic moments compared with the corresponding bulk values were clearly elucidated: ~15% for the spin magnetic moment and ~96 and ~53% for the orbital magnetic moments along the surface parallel and normal directions, respectively. [DOI: 10.1143/JJAP.47.2132]

KEYWORDS: X-ray magnetic circular dichroism, magnetic thin film, magnetic anisotropy, spin magnetic moment, orbital magnetic moment, superconducting magnet

1. Introduction

Enhancements of the magnetic moments of ultrathin films have extensively been investigated both theoretically^{1–7)} and experimentally^{8–12)} because of their importance in fundamental physics as well as technological applications to magnetic recording media. More recently, owing to the improvement of experimental techniques, the magnetic moments on nanorods,¹³⁾ nanoclusters¹⁴⁾ and atoms embedded in alkali metals¹⁵⁾ have also been studied. One of the most promising experimental methods for the determination of the magnetic moments in ultrathin films is X-ray magnetic circular dichroism (XMCD)¹⁶⁾ since it provides information on spin and orbital magnetic moments separately evaluated by applying so-called sum rules.^{17,18)}

There have already been reported extensive XMCD works concerning the enhancement of the orbital magnetic moment m_{orb} . Tischer *et al.*⁸⁾ performed a pioneering XMCD work on the enhancement of m_{orb} for >2 ML (monolayer) Co films on Cu(001) with respect to the effective spin magnetic moment $m_{\text{spin}}^{\text{eff}}$ by measuring *in situ* Co L-edge XMCD in a remanent magnetization state. From the thickness-dependent measurements, the enhancement of $m_{\text{orb}}/m_{\text{spin}}^{\text{eff}}$ for the surface Co atoms was estimated to be as much as ~100%. Weller *et al.*⁹⁾ reported the *ex situ* XMCD results for the Au/Co/Au ultrathin film at a magnetic field of 1 T and again concluded the enhancement of m_{orb} . Nakajima *et al.*¹⁰⁾ also showed the enhancement of m_{orb} in the Co/Pt multilayer system at magnetic fields of 1.1–2.0 T.

In contrast to the successful estimation of m_{orb} , the determination of the spin magnetic moment m_{spin} is typically more complex in the XMCD analysis. To avoid difficulty in the estimation of total magnetic moments by XMCD, Ney *et al.*¹²⁾ developed an excellent ultrahigh-vacuum (UHV) compatible superconducting quantum interference device (SQUID) magnetometer to determine the total magnetic moment of Co/Cu(001). They discussed the relative spin and orbital magnetic moments by combining the XMCD results with the SQUID results. The spin magnetic moment can however be evaluated directly by XMCD using the spin sum rule given as

$$m_{\text{spin}}^{\text{eff}} = m_{\text{spin}} + 7m_{\text{T}}, \quad (1)$$

where $m_{\text{spin}}^{\text{eff}}$ is obtained experimentally and m_{T} is the magnetic dipole moment. The difficulty in estimating m_{spin} by XMCD is caused mainly by the determination of m_{T} since m_{T} is typically not negligible in the ultrathin films or nanoclusters. To overcome the difficulty, Stöhr and König¹⁹⁾ proposed angle-dependent measurements of XMCD at saturation magnetization, which cancel the magnetic dipole term owing to the absence of the angle dependence of m_{spin} at saturation magnetization.

Saturation magnetization along the magnetically hard axis typically requires a high magnetic field of a few Tesla. Koide *et al.* designed and fabricated a high-magnetic-field XMCD system equipped with a UHV-compatible superconducting magnet,²⁰⁾ and reported the direct determination of both m_{spin} and m_{orb} for Co nanoclusters embedded in Au.¹⁴⁾ They performed *ex situ* XMCD measurements at a high magnetic field of ± 5 T, and successfully revealed the enhancements of both m_{spin} and m_{orb} .

In the present work, we have investigated the enhancements of m_{spin} and m_{orb} for submonolayer Co/Cu(001). In the previous work of the Co nanoclusters in Au,¹⁴⁾ the magnetic moments of the interface Co atoms were measured, while in the present study, those of the surface Co atoms were examined. The Co/Cu(001) system is one of the most basic examples for the investigation of surface magnetism. Although there have been many reports concerning >2 ML Co, direct determination of the magnetic moments of submonolayer Co/Cu(001) has not yet been performed because of the requirements of a high magnetic field and a very low temperature. For this purpose, we have designed and constructed a UHV-compatible XMCD system with a 7 T superconducting magnet and a liquid He cryostat. The system has been installed at Beamline 4B²¹⁾ of the synchrotron radiation facility UVSOR-II in Institute for Molecular Science (IMS). We have recorded the angle-dependent Co L_{III,II}-edge XMCD of 0.4 ML Co films grown epitaxially on Cu(001). The magnetization was confirmed to be saturated even along the hardest [001] axis of the surface normal. Through the analysis of the XMCD using the orbital

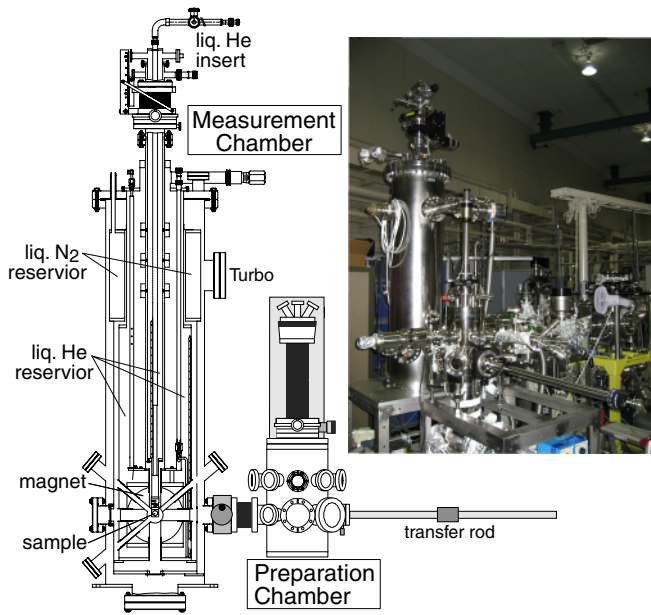


Fig. 1. (Color online) Schematic rear view and image of XMCD measurement system. The X-rays come from the back surface with a configuration parallel to a magnetic field. The liquid He reservoir with a 25L capacity is surrounded by a liquid nitrogen reservoir with a nominal 10L capacity.

and spin sum rules, we have consequently found enhancements of both m_{spin} and m_{orb} .

2. Design and Performance of XMCD System

In this work, we have designed and fabricated a new XMCD measurement system with a 7 T UHV-compatible superconducting magnet. The system consists of two separated UHV chambers for XMCD measurement and sample preparation. The schematic view and image of the system are depicted in Fig. 1. The sample preparation chamber is equipped with metal evaporators, reflection high-energy electron diffraction (RHEED) or low-energy electron diffraction and Auger electron spectroscopy (LEED/AES) optics, an ion gun, a sample-heating system, and so forth. The chamber is evacuated with a turbo molecular pump, a non-evaporation getter pump and a Ti sublimation pump. The base pressure is around 8×10^{-11} Torr.

The measurement chamber was constructed by JANIS Research Company. The system (model 7THM-ST-UHV) consists of a superconducting magnet and a variable temperature insert. The magnet is a 7 T (horizontal field) split multifilamentary NbTi superconducting magnet with a homogeneity of $\pm 0.5\%$ over a 1 cm diameter sphere. The sweep speeds are 1 T/min up to 5 T and 0.25 T/min from 5 to 7 T. A liquid helium reservoir with a 25 L capacity and a minimum of 12 h static hold time (24 h hold time without applying magnetic field) was used.

The sample cryostat has a built in heater and two calibrated Cernox thermometers plus a two-section high-efficiency continuous-flow-type liquid helium transfer line. This offers the lowest sample temperatures of ~ 4.8 K for accumulated He and ~ 3.8 K for pumped He. The sample cryostat can be rotated 360° , allowing us to measure angle-dependent XMCD spectra. A sample holder is a hexagonal Mo with a screw. For future magneto-optical Kerr effect

(MOKE) and/or laser-induced photoemission MCD measurements,^{22,23} the chamber possesses several ICF70 viewing ports accessible to the center of the magnet. These ports enable the MOKE measurements with the polar and transverse configurations. The chamber is pumped with a turbo molecular pump, which can be shut down during liquid He insertion. The base pressure is below 2×10^{-10} Torr at the ionization gauge position and should be much lower at the sample position.

3. XMCD Measurements

The XMCD system was installed at Beamline 4B²¹⁾ of UVOSR-II in IMS. The beamline is a bending-magnet soft X-ray station equipped with a varied line spacing grating monochromator, which covers the photon energies of 25–1000 eV. The circularly polarized X-rays were obtained by adjusting the vertical aperture upstream of the first mirror. In the present experiment, negative-helicity X-rays were used. The circular polarization factor was estimated to be $P_c = 0.85 \pm 0.03$ from the storage ring parameters, which was verified by the XMCD measurement of a standard sample. The energy resolving power was $E/\Delta E \sim 700$ at $E = 700$ eV.

A Cu(001) single crystal was cleaned in the preparation chamber by repeated cycles of Ar^+ bombardment (900 V) and annealing at ~ 800 K. Cleanliness and order were verified by X-ray absorption spectroscopy (XAS) and RHEED, respectively. A submonolayer Co film was subsequently deposited on a clean Cu(001) surface at < 310 K from a commercial evaporator with a growth rate of 0.2 ML/min. The Co thickness can be monitored with the RHEED oscillation for > 1 ML Co. In the present submonolayer case, the thickness was estimated to be 0.4 ML by the subsequent XAS measurements of 0.4 and 3.0 ML Co.

Co $L_{\text{III,II}}$ -edge circularly polarized X-ray absorption spectra were recorded with a total electron yield mode by detecting a drain current from the sample. The spectra were taken at 6.0 K by switching the magnetic fields H , leaving the negative photon helicity unchanged. A magnetization curve along the magnetically hardest [001] axis was first measured in order to estimate the minimum magnetic field H_s at which the perpendicular magnetization is saturated. Here, only the Co L_{III} -edge region was recorded. Subsequently, angle-dependent Co $L_{\text{III,II}}$ -edge XMCD spectra were taken at the X-ray incidence polar angles θ_i of 60° (grazing incidence) and 0° (normal incidence). The X-ray propagation direction is always parallel to \mathbf{H} in the present setup. The $\theta_i = 60^\circ$ and 0° spectra were recorded at $H = \pm 0.1$ and ± 5.0 T, respectively.

4. Results and Discussion

It is known that the present sample shows the magnetically easy axis of [110] (within the surface plane) and the hardest axis of [001] (surface normal).^{8,11,12,24,25} Moreover, Co is found to grow in a layer-by-layer fashion, and a 0.4 ML Co film shows mostly single-layer large islands with a small amount of the second layer.²⁴ This is in good contrast to the previous Au/Co/Au system,¹⁴ where most Co clusters form a double layer and the magnetically easy axis is perpendicular to the surface. The present growth conditions (the substrate temperature of < 310 K and the

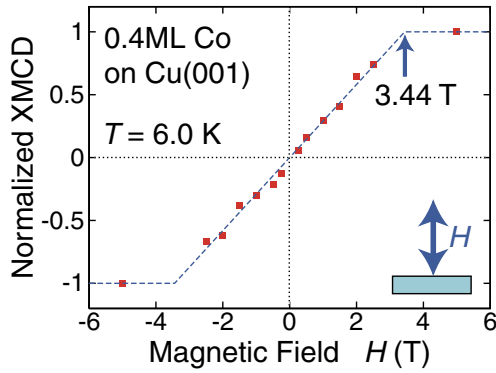


Fig. 2. (Color online) Magnetization curve of 0.4 ML Co on Cu(001) at 6.0 K along surface normal [001] direction, recorded as Co L_{III} XMCD intensity. The red points are the experimental data, and the blue dashed line is the fitted result using the second-order approximation of the magnetic anisotropy energy.

growth rate of 0.2 ML/min) indicate that the intermixing with Cu is not significant in contrast to the growth at higher temperatures.^{25–27}

Figure 2 shows the magnetization curve of 0.4 ML Co on Cu(001) at 6.0 K along the [001] direction. The magnetization is scaled using the area of the Co L_{III} peak. The magnetization is found to increase linearly up to $H = \pm 2.5$ T, while the magnetizations at $H = \pm 5.0$ T are apparently weaker than those expected from the extrapolated linear line. A magnetic anisotropy energy E_a of a magnetic thin film at a perpendicular external magnetic field is phenomenologically expressed in the second-order approximation as

$$E_a = \left(\frac{1}{2\mu_0} N M_s^2 - K_2 \right) \cos^2 \theta_M - M_s H \cos \theta_M, \quad (2)$$

where μ_0 is the permeability of vacuum, M_s the saturated magnetization, N the demagnetizing factor ($N = 1$ for an infinitely wide film), and K_2 the second-order magneto-crystalline and/or magnetoelastic anisotropic constant. The perpendicular component of magnetization, $M_s \cos \theta_M$, is obtained by minimizing E_a in eq. (2). This yields a linear function up to H_s , while it turns flat above H_s . By fitting the experimentally obtained data points ($|H| < 2.5$ T) with a linear function, H_s is estimated to be ~ 3.4 T. The magnetic fields of ± 5 T are thus confirmed to saturate the magnetization even along the [001] axis.

Figure 3 depicts the Co L_{III,II}-edge circularly polarized X-ray absorption spectra, μ^+ and μ^- , taken at $\theta_i = 60$ and 0° . μ^+ and μ^- denote those for the X-ray helicities parallel and antiparallel to the electron spins in the specimen, respectively. The spectra are obtained from a linear background at the preedge energy and a subsequent normalization with the edge jump at the postedge energy. Self-absorption correction²⁸⁾ is performed for all the spectra by assuming a perfectly flat film. This procedure is however not at all important since the present Co thickness of 0.4 ML is small. The XMCD spectra are resultantly obtained by the subtraction of the two circularly polarized spectra and the normalization with a polarization factor. In the case of the $\theta_i = 60^\circ$ spectra, the magnetization \mathbf{M} is still lying flat along [110] with a negligibly small perpendicular component due

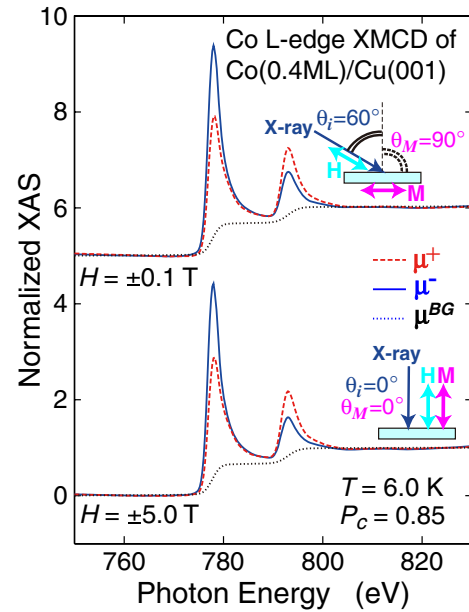


Fig. 3. (Color online) Co L_{III,II}-edge circularly polarized X-ray absorption spectra of 0.4 ML Co on Cu(001) at 6.0 K recorded with total electron yield mode (sample drain current). In the top spectra, magnetization is along the easy axis of [110] within the surface plane ($\theta_M = 90^\circ$), and the X-ray incidence and the external magnetic field (± 0.1 T) are directed to $\theta_i = 60^\circ$ from the surface normal. In the bottom spectra, the magnetization, the X-ray incidence and the external magnetic field (± 5.0 T) are all aligned to the [001] hardest axis: $\theta_M = 0^\circ$ and $\theta_i = 0^\circ$. The solid blue and dashed red lines correspond to $\mu^+(\theta_M)$ and $\mu^-(\theta_M)$, respectively, while the black dotted lines are the background absorption μ^{BG} . The spectra were self-absorption-corrected, although the effect is essentially negligible for the present thickness.

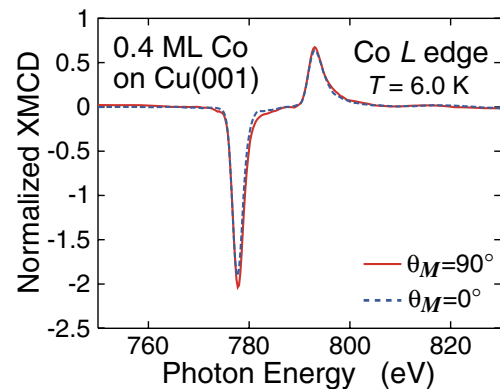


Fig. 4. (Color online) Co L_{III,II}-edge XMCD spectra of 0.4 ML Co on Cu(001) at 6.0 K for the magnetization parallel ($\theta_M = 90^\circ$) and perpendicular ($\theta_M = 0^\circ$) to the surface.

to a weak magnetic field of $H = \pm 0.1$ T. Thus, the angle between \mathbf{M} and the X-ray propagation direction is 30° . The XMCD spectrum is normalized with a factor of $P_c \cos 30^\circ$. On the other hand, the XMCD spectrum along the [001] axis is taken at normal X-ray incidence at $H = \pm 5.0$ T ($\mathbf{H} \parallel [001]$). The magnetization saturation is verified. The spectrum is normalized with P_c . Figure 4 shows the XMCD spectra for $\theta_M = 90$ and 0° , where θ_M denotes the polar angle of \mathbf{M} . Although the two XMCD spectra are not very different from each other, small dissimilarities can clearly be seen around the L_{III,II}-edge peaks, indicating small anisotropic features in the present submonolayer film.

$m_{\text{orb}}(\theta_M)$ and $m_{\text{spin}}^{\text{eff}}(\theta_M)$ are obtained using the sum rules^{17,18)} as

$$m_{\text{orb}}(\theta_M) = \frac{2n_h\mu_B}{3I_{\text{av}}} \int_{L_{\text{III}}+L_{\text{II}}} \Delta\mu dE \quad (3)$$

and

$$m_{\text{spin}}^{\text{eff}} = \frac{n_h\mu_B}{3I_{\text{av}}} \left(\int_{L_{\text{III}}} \Delta\mu dE - 2 \int_{L_{\text{II}}} \Delta\mu dE \right), \quad (4)$$

where n_h is the d -hole number, μ_B the Bohr magneton, and $\Delta\mu$ the experimentally obtained XMCD spectrum given in Fig. 4. The normalization factors I_{av} correspond to the average $L_{\text{III,II}}$ peak area ($2p \rightarrow 3d$) transition intensity) and is given as

$$I_{\text{av}} = \int_{L_{\text{III}}+L_{\text{II}}} \left(\frac{\mu^+ + \mu^-}{2} - \mu^{\text{BG}} \right) dE, \quad (5)$$

where μ^{BG} is the background absorption spectrum expressed by the two step functions (see Fig. 3 for μ^+ , μ^- , and μ^{BG}). I_{av} is proportional to n_h .

To determine the absolute numbers of the magnetic moments, we first estimate the proportional factor of n_h/I_{av} using a standard XMCD spectrum of 3.0 ML Co on Cu(001) at 6.5 K, where $n_h = 2.50$ is assumed.⁵⁾ The XMCD spectra of 3.0 ML Co/Cu(001), which were taken in a similar grazing geometry, yield $m_{\text{spin}}^{\text{eff}} = 1.75 \pm 0.10 \mu_B$ and $m_{\text{orb}} = 0.21 \pm 0.05 \mu_B$. Those results are consistent with those previously reported,¹¹⁾ namely, $m_{\text{spin}} = 1.77 \pm 0.10 \mu_B$ and $m_{\text{orb}} = 0.24 \pm 0.05$ for 2.1 ML Co/Cu(001).²⁹⁾

In 0.4 ML Co, we obtain the d -hole numbers $n_h(90^\circ) = 2.56 \pm 0.15$ and $n_h(0^\circ) = 2.48 \pm 0.15$, implying that the d -hole number of 0.4 ML Co is almost angle-independent of and also similar to that of 3 ML Co. Subsequently, we evaluate the magnetic moments of 0.4 ML Co using the sum rules to be $m_{\text{orb}}(90^\circ) = 0.29 \pm 0.05 \mu_B$, $m_{\text{orb}}(0^\circ) = 0.23 \pm 0.05 \mu_B$, $m_{\text{spin}}^{\text{eff}}(90^\circ) = 1.86 \pm 0.10 \mu_B$, and $m_{\text{spin}}^{\text{eff}}(0^\circ) = 1.65 \pm 0.10 \mu_B$.

Consequently, m_{spin} can be estimated by subtracting the m_T term in eq. (1). Stöhr and König¹⁹⁾ proposed important formulas in the angle-dependent XMCD measurement as

$$m_{\text{orb}}(\theta_M) = m_{\text{orb}}^\perp \cos^2 \theta_M + m_{\text{orb}}^\parallel \sin^2 \theta_M, \quad (6)$$

$$m_T(\theta_M) = m_T^\perp \cos^2 \theta_M + m_T^\parallel \sin^2 \theta_M, \quad (7)$$

and

$$m_T^\perp + 2m_T^\parallel = 0, \quad (8)$$

where the superscripts \perp and \parallel denote the moment directions perpendicular and parallel to the surface, respectively. By using the numerical values obtained above, we can eventually evaluate the magnetic moments. The magnetic dipole terms are given as $m_T^\parallel = 0.010 \pm 0.05 \mu_B$ and $m_T^\perp = -0.020 \pm 0.05 \mu_B$. The spin magnetic moment of $m_{\text{spin}} = 1.79 \pm 0.10 \mu_B$ is around 12% larger than that of bulk hcp Co ($m_{\text{spin}}^{\text{bulk}} = 1.55 \mu_B$), and the orbital magnetic moments of $m_{\text{orb}}^\parallel = 0.29 \pm 0.05 \mu_B$ and $m_{\text{orb}}^\perp = 0.23 \pm 0.05 \mu_B$ are much more significantly greater than the bulk value of $m_{\text{orb}}^{\text{bulk}} = 0.15 \mu_B$.

Tischer *et al.*⁸⁾ reported $m_{\text{orb}}^\parallel/m_{\text{spin}}^{\text{eff}} \sim 0.10$ for 2 ML Co. The present result is $m_{\text{orb}}^\parallel/m_{\text{spin}}^{\text{eff}} = 0.16 \pm 0.02$, which is small but markedly larger than their result owing to a smaller Co thickness in the present case. From the thick-

ness dependent XMCD measurements, they estimated $m_{\text{orb}}^\parallel/m_{\text{spin}}^{\text{eff}} \sim 0.19$ for the surface Co atoms, while they estimated $m_{\text{orb}}^\parallel/m_{\text{spin}}^{\text{eff}} \sim 0.141$ from their theoretical calculation. The agreement with the present result is acceptable. Srivastava *et al.*¹¹⁾ reported $m_{\text{orb}}^\parallel = 0.24 \pm 0.05 \mu_B$ and $m_{\text{spin}} = 1.77 \pm 0.10 \mu_B$ for 2.1 ML Co/Cu(001).²⁹⁾ The m_{spin} and m_{orb}^\parallel values are similar to the present results within the error bars. On the other hand, Ney *et al.*¹²⁾ gave, by SQUID measurement of >2 ML Co/Cu(001), the total magnetic moment $m_{\text{tot}}^\parallel = m_{\text{spin}} + m_{\text{orb}}^\parallel$ of $1.87 \pm 0.03 \mu_B$ for 2 ML Co, which is slightly smaller than the present 0.4 ML result of $m_{\text{tot}}^\parallel = 2.08 \pm 0.15 \mu_B$.

There have also been reported theoretical estimations for the spin magnetic moment of monolayer Co/Cu(001): $m_{\text{spin}} = 1.71 \mu_B$,⁷⁾ $1.78 \mu_B$,⁴⁾ and $1.85 \mu_B$.^{1,5)} Although the theoretical estimations are rather scattered depending on the calculation method and the employed lattice constant, 10–20% enhancement of m_{spin} compared with the bulk value is in fairly good agreement with the present finding. Hjortstam *et al.*⁵⁾ also evaluated the orbital magnetic moment of $m_{\text{orb}}^\perp = 0.261 \mu_B$, assuming perpendicular magnetization for calculational simplicity, which is consistent with the present result of $m_{\text{orb}}^\perp = 0.23 \pm 0.05 \mu_B$.

5. Conclusions

In this work, we have designed and constructed a new UHV-compatible XMCD measurement system, by which the XMCD spectra can be recorded at a magnetic field of maximum ± 7 T and at a sample temperature of 4.8 K (accumulated He) or 3.8 K (pumped He). By using this system, magnetic properties of submonolayer (0.4 ML) Co grown epitaxially on Cu(001) have been investigated. The angle-dependent XMCD spectra for the saturated magnetization taken at 6.0 K allowed us to evaluate spin and orbital magnetic moments separately along the surface parallel and perpendicular directions. Their enhancements have clearly been determined and compared with the corresponding bulk values: $\sim 15\%$ for the spin magnetic moment and ~ 96 and $\sim 53\%$ for the orbital magnetic moments along the surface parallel and perpendicular directions, respectively. The enhancements of the orbital and spin magnetic moments for the submonolayer Co atoms are as a whole consistent with the previous theoretical and experimental estimations.

Acknowledgements

We would like to express our greatest thanks to Dr. M. Jirmanus of JANIS Research Company, Inc., MA, U.S.A. and Mr. Y. Miyasaka of MyScience, Tokyo, Japan for their sincere support for our many difficult requests concerning the performance of the superconducting magnet and the liquid He variable temperature insert, to Professor E. Shigemasa, Mr. E. Nakamura and other UVSOR staff members of IMS for their tremendous efforts in the installation of the present system at Beamline 4B of UVSOR-II, to staff members of Equipment Development Center in IMS for the manufacturing of the sample holders, and to Professor T. Koide of Photon Factory of Institute of Materials Structure Science, Tsukuba, Japan for his advice regarding our XMCD system. The authors are also grateful for the financial supports of Grant-in-Aid for Scientific

Research (No. 16710093) from the Ministry of Education, Culture, Sports, Science and Technology (MEXT) and from the Japan Society for the Promotion of Science (No. 19201023). The present work was also supported by the Nanotechnology Network Project from MEXT.

- 1) O. Eriksson, A. M. Boring, R. C. Albers, G. W. Fernando, and B. R. Cooper: *Phys. Rev. B* **45** (1992) 2868.
- 2) S. Brügel: *Phys. Rev. Lett.* **68** (1992) 851.
- 3) R. Wu, D. Wang, and A. J. Freeman: *Phys. Rev. Lett.* **71** (1993) 3581.
- 4) R. Wu and A. J. Freeman: *J. Appl. Phys.* **79** (1996) 6500.
- 5) O. Hjortstam, J. Trygg, J. M. Wills, B. Johansson, and O. Eriksson: *Phys. Rev. B* **53** (1996) 9204.
- 6) A. M. N. Niklasson, B. Johansson, and H. L. Skriver: *Phys. Rev. B* **59** (1999) 6373.
- 7) R. Pentcheva and M. Scheffler: *Phys. Rev. B* **61** (2000) 2211.
- 8) M. Tischer, O. Hjortstam, D. Arvanitis, J. Hunter Dunn, F. May, K. Baberschke, J. Trygg, J. M. Wills, B. Johansson, and O. Eriksson: *Phys. Rev. Lett.* **75** (1995) 1602.
- 9) D. Weller, J. Stöhr, R. Nakajima, A. Carl, M. G. Samant, C. Chappert, R. Mégy, P. Beauvillain, P. Veillet, and G. A. Held: *Phys. Rev. Lett.* **75** (1995) 3752.
- 10) N. Nakajima, T. Koide, T. Shidara, H. Miyauchi, H. Fukutani, A. Fujimori, K. Iio, T. Katayama, M. Nyvlt, and Y. Suzuki: *Phys. Rev. Lett.* **81** (1998) 5229.
- 11) P. Srivastava, F. Wilhelm, A. Ney, M. Farle, H. Wende, N. Haack, G. Ceballos, and K. Baberschke: *Phys. Rev. B* **58** (1998) 5701.
- 12) A. Ney, P. Pouloupoulos, M. Farle, and K. Baberschke: *Phys. Rev. B* **62** (2000) 11336.
- 13) P. Gambardella, A. Dallmeyer, K. Maiti, M. C. Malagoli, S. Rusponi, P. Ohresser, W. Ebergardt, C. Carbone, and K. Kern: *Phys. Rev. Lett.* **93** (2004) 077203.
- 14) T. Koide, H. Miyauchi, J. Okamoto, T. Shidara, A. Fujimori, H. Fukutani, K. Amemiya, H. Takeshita, S. Yuasa, T. Katayama, and Y. Suzuki: *Phys. Rev. Lett.* **87** (2001) 257201.
- 15) P. Gambardella, S. S. Dhesi, S. Gardonio, C. Grazioli, P. Ohresser, and C. Carbone: *Phys. Rev. Lett.* **88** (2002) 047202.
- 16) C. T. Chen, F. Sette, Y. Ma, and S. Modesti: *Phys. Rev. B* **42** (1990) 7262.
- 17) B. T. Thole, P. Carra, F. Sette, and G. van der Laan: *Phys. Rev. Lett.* **68** (1992) 1943.
- 18) P. Carra, B. T. Thole, M. Altarelli, and X. Wang: *Phys. Rev. Lett.* **70** (1993) 694.
- 19) J. Stöhr and H. König: *Phys. Rev. Lett.* **75** (1995) 3748.
- 20) T. Koide, T. Shidara, and H. Fukutani: *Rev. Sci. Instrum.* **63** (1992) 1462.
- 21) T. Gejo, Y. Takata, T. Hatsui, M. Nagasono, H. Oji, N. Kosugi, and E. Shigemasa: *Chem. Phys.* **289** (2003) 15.
- 22) T. Nakagawa and T. Yokoyama: *Phys. Rev. Lett.* **96** (2006) 237402.
- 23) T. Nakagawa, T. Yokoyama, M. Hosaka, and M. Katoh: *Rev. Sci. Instrum.* **78** (2007) 023907.
- 24) U. Ramsperger, A. Vaterlaus, P. Pfäffli, U. Maier, and D. Pescia: *Phys. Rev. B* **53** (1996) 8001.
- 25) P. Pouloupoulos, P. J. Jensen, A. Ney, J. Lindner, and K. Baberschke: *Phys. Rev. B* **65** (2002) 064431.
- 26) J. Fassbender, R. Allenspach, and U. Dürig: *Surf. Sci.* **383** (1997) L742.
- 27) X.-D. Liu, T. Iimori, K. Nakatsuji, and F. Komori: *Appl. Phys. Lett.* **88** (2006) 133102.
- 28) R. Nakajima, J. Stöhr, and Y. U. Idzerda: *Phys. Rev. B* **59** (1999) 6421.
- 29) Their m_{spin} was estimated by subtracting the theoretically evaluated m_{T} and further adding the theoretical sp-band contribution.